Available online at www.eccomasproceedia.org
Eccomas Proceedia SMART (2023) 789-799

ECCOMAS
Proceedia

X ECCOMAS Thematic Conference on Smart Structures and Materials
SMART 2023
D.A. Saravanos, A. Benjeddou, N. Chrysochoidis and T. Theodosiou (Eds)

DISPLACEMENT-RATIO-BASED PROBABILISTIC DAMAGE DETECTION OF BRIDGES USING FE MODEL UPDATE

YOSHIYUKI YAJIMA*, MURTUZA PETLADWALA*, TAKAHIRO KUMURA*, AND CHUL-WOO KIM†

*Visual Intelligence Research Laboratories
NEC Corporation
Kawasaki, 211-8666 Kanagawa, Japan
e-mail: yoshiyuki-yajima@nec.com

† Department of Civil and Earth Resources Engineering
Kyoto University
Katsura Campus, 615-8540 Kyoto, Japan
e-mail: kim.chulwoo.5u@kyoto-u.ac.jp

Abstract. This paper presents a probabilistic damage detection for bridges from displacement ratio through the finite element (FE) model update. Live-load displacement is crucial to understand the integrity of bridges while it depends on loads. Instead, the displacement ratio is useful because it is independent of loads. This study focuses on probability density functions (PDFs) of displacement ratio. Using the PDFs, the feasibility of detecting damage in bridge girders is investigated in an in-house experiment with a model bridge. PDFs of stiffness for each half span of the girder are estimated from measured displacement ratio PDFs based on the FE model update process. In the damage scenario, estimated PDFs of stiffness are significantly shifted to those in the intact scenario. Focusing on these changes in PDFs makes damage detection possible with an approximate estimation of the damage location.

Key words: Anomaly detection, Bridge health monitoring, Live-load displacement, Finite element model, Bayesian model update

Peer-review under responsibility of the organizing committee of SMART 2023.
doi: 10.7712/150123.9832.450726

1 INTRODUCTION

Damaged and aged bridges are increasing in many countries, however, visual inspection is a major approach in bridge maintenance yet The visual inspection faces difficulties in damage detection unless inspectors are able to approach the damage suspected places easily. Therefore, developing monitoring technologies and systems to assess bridge integrity is a keen issue.

Vertical displacement (hereafter, displacement) caused by traffic load is important physical property to infer bridge health conditions. If the flexural rigidity partially decreases due to damage in a girder, live-load displacement at positions close to the damage becomes more significant than those far from the damage. It was confirmed in simulations [1] and experiments [2]. These studies suggest possibilities of damage detection focusing on changes in displacement.

Displacement depends on traffic situations, i.e., live-load, and it needs to know the load to utilize the displacement in damage detection. In practice, however, measuring bridge load is challenging because of additional sensors, installation costs, and sophisticated technologies like Bridge-Weigh-in-Motion. Therefore, information on external loads is necessary to identify any changes in bridge integrity using displacement information on external loads.

Some studies proposed a way to solve this issue using ratio-based features related to displacement measured at different positions [3, 4]. The displacement y for a simple beam with the flexural rigidity EI and the load P is theoretically $y \propto P/EI$. Hence, taking a ratio of displacement reduces a factor of P, whereas EI is not eliminated if it is non-uniform due to partial damage.

The existing study [4] using ratio-based features needs the supervised learning of known damage to understand bridge integrity (i.e., physical condition) and localization of damage. However, it is almost impossible to get ground-truth data on damage in practical cases because damage is unknown before visual inspections. Methods that estimate the condition of the bridge without pre-training processes are useful in actual monitoring.

In terms of structural integrity estimation, the finite element (FE) model update [5, 6] adopting Bayesian inference, Bayesian model update [7, 8, 9, 10], is a powerful technique. The FE model update reduces the discrepancy between the results of measurements and FE model simulations by calibrating structural parameters in the FE model. As a result, the structural integrity of bridges can be estimated from calibrated parameters. The Bayesian model update further estimates the posterior probability of structural parameters based on observations. Regarding Bayesian inference, posterior probability distributions are estimated from prior probability distributions and measurement results. Probabilistic quantities enable us to consider error and uncertainty in measurement data. Furthermore, detecting changes in structural parameters PDFs from a reference condition makes damage detection possible [11, 12]. This paper proposes a probabilistic damage detection method through FE model update using PDFs of the displacement ratio.

2 DAMAGE DETECTION METHOD

The process of the proposed damage detection method is shown in Figure 1. From measurements of displacement, PDFs of displacement ratio are derived. In parallel, displacement at measurement positions is simulated in the FE model with many sets of structural parameters under less calculation time. A surrogate model is developed to estimate displacement ratio at structural parameters specified arbitrarily. A combination of displacement ratio PDFs and the surrogate model, PDFs of structural parameters are estimated according to the FE model update process. Damage is detected by analyzing the estimated PDFs.

PDFs of a displacement ratio are derived as follows. For each vehicle-passing event, the maximum displacements obtained by displacement transducers at positions i and j are identified after the time-averaging filter for data. Displacement data around the time at the local maxima are extracted in the range of $\pm\Delta t$. When the sampling frequency of the displacement transducer is f_s, the total number of samples in the extracted displacement data is $1 + 2f_s\Delta t$. For each sampled displacement, the displacement ratio of transducers at j to i is derived, i.e., for the k-th sample of the extracted displacement data (here $k = 1, 2, \ldots, 1 + 2f_s\Delta t$),

$$r_k = (y_{j,k} - y_{i,k})/y_{i,k} \tag{1}$$

is derived, where r_k is a displacement ratio sample, $y_{i,k}$ and $y_{j,k}$ are the sampled displacement at position i and j, respectively. From the histogram of displacement ratios $\{r_k\}$, its PDF is estimated using the Kernel Density Estimation.

In the FE model update, the Metropolis–Hastings Markov Chain Monte Carlo (MCMC) algorithm is adopted as a sampling method. Each step in the MCMC process samples sets of structural parameters based on a random walk in the space of structural parameters defined by the prior distributions. Sampled parameter sets are judged whether they are acceptable based on the acceptance probability α. Here, α is defined as

$$\alpha = \min\left\{1, \frac{p(r_2|\boldsymbol{\theta}_2)}{p(r_1|\boldsymbol{\theta}_1)}\right\}, \tag{2}$$

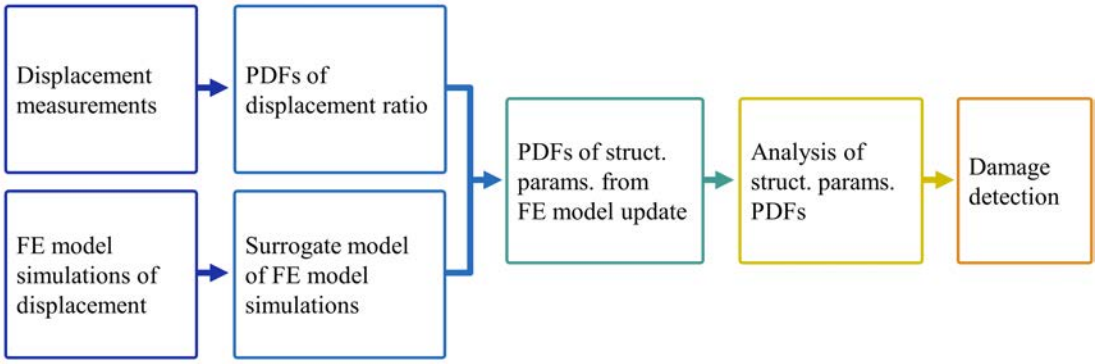

Figure 1: Flow of the proposed damage detection method.

where $\boldsymbol{\theta}_n$ $(n = 1, 2)$ is a set of considered structural parameters, $r_n|\boldsymbol{\theta}_n$ is the displacement ratio at given $\boldsymbol{\theta}_n$ estimated by the surrogate model, and $p(.)$ is the PDF of displacement ratio. If α is larger than a random number u generated by the uniform distribution $\mathcal{U}[0, 1]$, $\boldsymbol{\theta}_2$ is accepted and $\boldsymbol{\theta}_1$ is updated to $\boldsymbol{\theta}_2$. In the next step, new $\boldsymbol{\theta}_2$ is sampled as $\boldsymbol{\theta}_2 = \boldsymbol{\theta}_1 + \boldsymbol{w}$, where each element of $\boldsymbol{w}$ is a random number generated by Gaussian noise. PDFs of structural parameters are estimated by obtaining histograms of accepted $\boldsymbol{\theta}_2$ along each structural parameter axis (i.e., marginal distributions). Detailed settings are described in Section 4.2.

This paper attempts to detect damage in a girder, which changes flexural rigidity EI. For simplicity, we regard any changes in EI as those in Young's modulus E. In other words, girder damage is detected from detecting changes in PDFs of E, and significance of changes in PDFs of E indicates quantitative damage severity.

3 DISPLACEMENT RATIO

3.1 LOAD INDEPENDENCY

An in-house experiment using a model bridge is carried out to verify the validity of the proposed method. We firstly check the load independency of displacement ratio PDFs. The model bridge used in the in-house experiment is a 5.4 m-long "I"-shaped simply supported steel beam bridge, as shown in Figure 2 (a). Live-load displacement is measured with displacement transducers under a traveling model vehicle. Displacement transducers are installed at locations D1-D5, shown in Figure 2 (b).

A pilot experiment is carried out to examine a PDF of displacement ratio that can be used for the FE model update and damage detection. In the pilot experiment, the mass of the model vehicle is set as 56 and 61 kg. Vehicle velocities are 0.66 and 0.86 m/s. The vehicle travels in 10 round trips for each vehicle mass and velocity setting.

Displacement data obtained at D1 and D5 are used in the pilot investigation, i.e., $i = \mathrm{D1}$ and $j = \mathrm{D5}$ in Equation (1). Displacement data around the time at the local maxima are extracted in the range of ± 0.5 seconds. Figures 3 (a) and (b) show histograms of extracted displacement around maximum value at D1 and D5, which are normalized so that the total area is unity. The bimodality in these histograms corresponds to the two settings of the vehicle masses. Figure 3 (c) shows normalized histograms and estimated PDFs of the displacement ratio of D5 to D1. According to this result, the bimodality is completely eliminated by taking the ratio of displacements.

3.2 ACTUAL BRIDGE CASE

Another pilot experiment is carried out at an actual Gerber-type steel girder bridge. Displacement data is acquired with displacement transducers installed at two positions between an internal hinge point of the Gerber beam as shown in Figures 4 (a) and (b). Measurement time is for 95 minutes and a total of 89 vehicle-passing events are used in the analysis. The displacement ratio is derived in the same way as described above.

Figure 4 (c) shows the PDF of the displacement ratio measured in the actual bridge. During

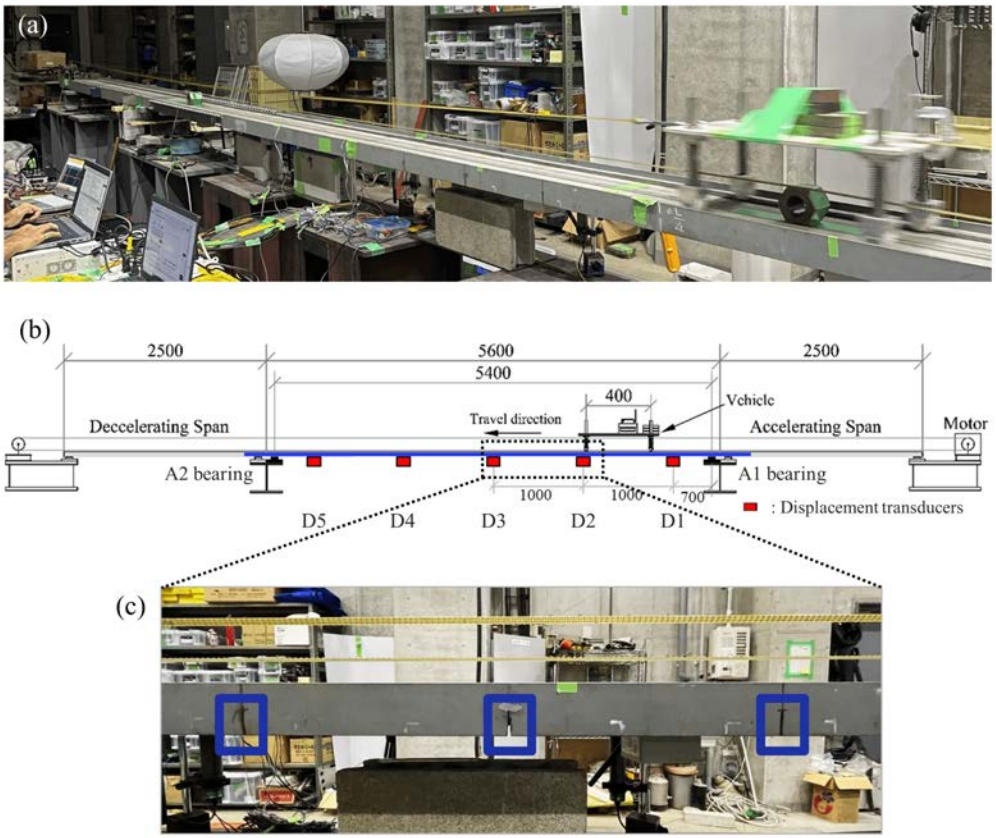

Figure 2: (a) Model bridge used in the in-house experiment, (b) Dimensions of the model bridge and locations of installed displacement transducers (elevation view), and (c) Three saw cuts in the girder as artificial damages.

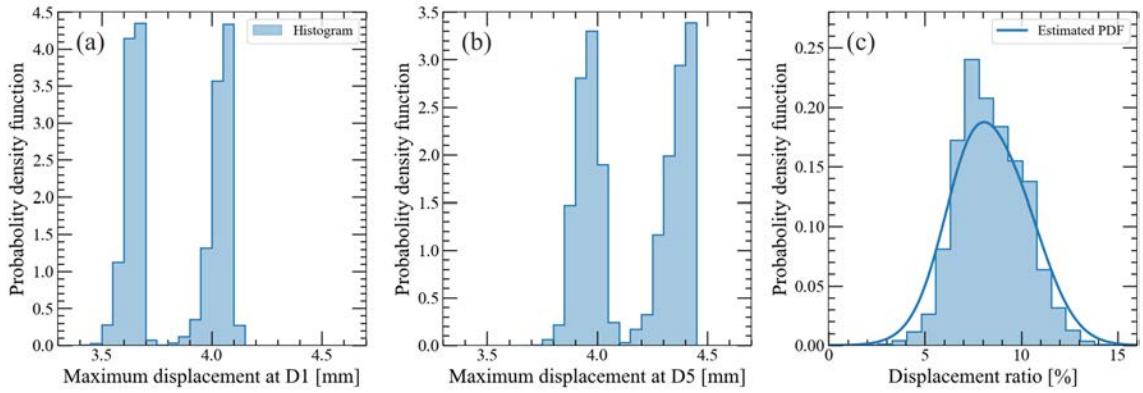

Figure 3: Normalized histograms (so that its total area is unity) of maximum displacement (a) at D1, (b) at D5, and (c) those of displacement ratio of D5 to D1 measured in the pilot experiment with a model bridge. Solid lines in (c) are estimated PDFs from the Kernel Density Estimation.

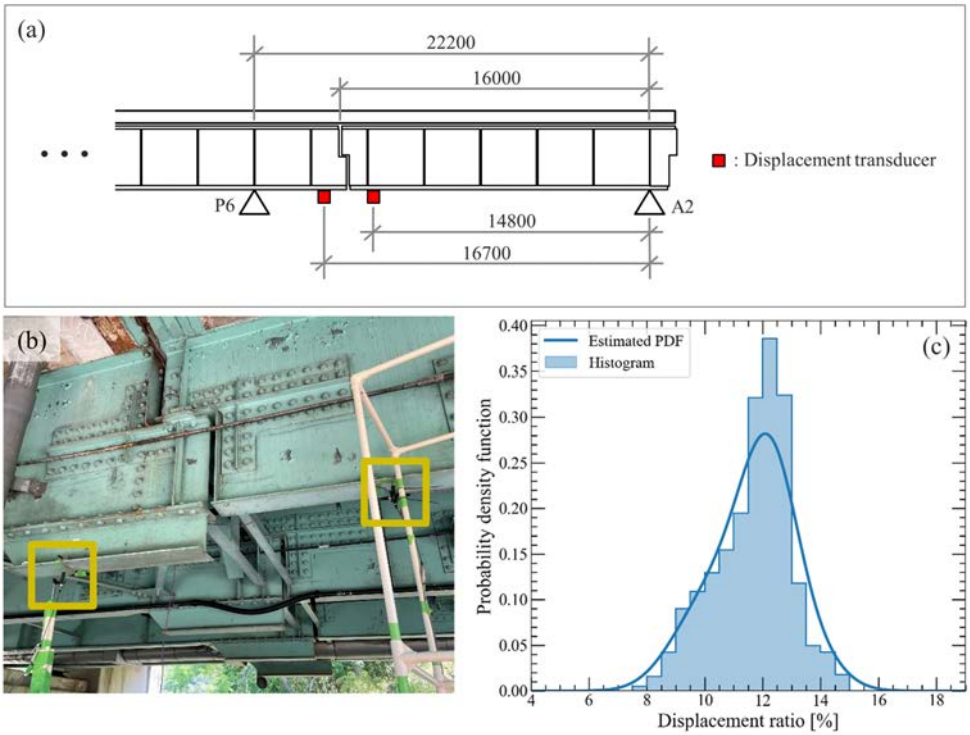

Figure 4: (a) Dimensions of an actual Gerber-type steel girder bridge and positions of installed displacement transducers (elevation view). (b) Installation of transducers highlighted by yellow squares in an actual bridge. (c) The normalized histogram and estimated PDF of displacement ratio derived in the actual bridge.

the measurement, different types of trucks, with axle distances from 5-m long to 12-m long, were observed using traffic cameras. Even in such a situation, the PDF of displacement ratio shows unimodality as shown in Figure 4 (c). Moreover, its expectation of around 10% and the standard deviation of around 5% are comparable to results obtained in the in-house experiment with the model bridge (Figure 3 (c)), while the displacement ratio depends on many factors such as measurement locations and structural properties. This result suggests that the PDF of displacement ratio is applicable for bridge structural health monitoring (BSHM).

3.3 DAMAGE SCENARIO

To examine differences in displacement ratio PDFs between the intact and damage scenario, an in-house experiment using the model bridge is carried out. In the model bridge, cracks on the girder are reproduced by three saw cuts, as shown in Figure 2 (c), which decrease the flexural rigidity by 11% [13]. These cuts are approximately between D2 and D3 (cf. Figure 2 (b)) with a length of 30 mm and width of 2.5 mm. This paper refers to the bridge condition with the saw cuts as the “damage scenario”, and the “intact scenario” is reproduced by reinforcing the saw cuts with additional steel plates.

In this experiment, the vehicle setting is changed to increase the efficiency of the experiment.

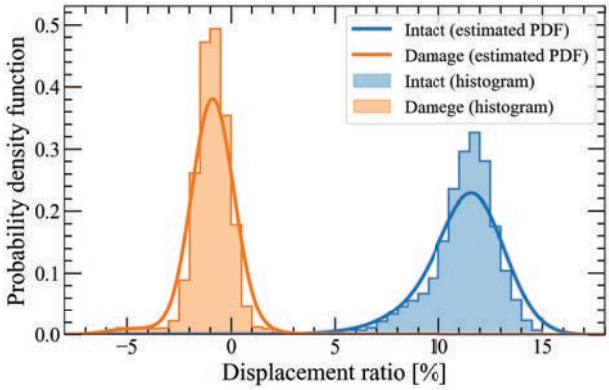

Figure 5: Normalized histogram and estimated probability density functions of displacement ratio in the intact and damage scenarios.

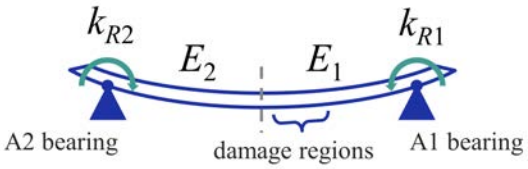

Figure 6: Adopted structural parameters in the FE model.

One pattern mass (25 kg) and higher velocities (0.86, 1.0, and 1.2 m/s) settings are adopted. In each mass, velocity, and bridge scenario, the vehicle travels in 40 round trips. The displacement ratio is derived using displacement transducers at D2 and D4, i.e., $i = \mathrm{D2}$ and $j = \mathrm{D4}$ in Equation (1).

Figure 5 shows the normalized histograms and estimated PDFs of the displacement ratio in each scenario. The PDF in the damage scenario shows a distinct difference from that in the intact scenario. The displacement ratio in the damage scenario decreases by 13% more than in the intact scenario. This is because deflection at D2 is larger than at D4 in the damage scenario due to the saw cuts around D2 and D3. The displacement ratio detects partial changes in the flexural rigidity. According to this result, displacement ratio PDFs can be applied for damage detection.

4 FE MODEL UPDATE PROCESS

The FE model is developed using the software "Midas Civil". The model consists of 270 beam elements. As structural parameters, Young's modulus for each half span of the girder (E_1 and E_2) and rotational spring stiffness at bearings (k_{R1} and k_{R2}), which determine the boundary condition are adopted as shown in Figure 6. This paper expresses decreased flexural rigidity by saw cuts as decreased Young's modulus.

4.1 SIMULATION SETUP

The ranges of each structural parameter are defined as follows. For E_1 and E_2, the upper and lower limit is set as $+10\%$ and -25% of the nominal value for steel (2.05×10^8 kN/m^2), respectively. The upper limit is a relatively narrow margin because no corresponding damage and aging increases the flexural rigidity. About the lower limit, the flexural rigidity of the model bridge decreases by 25% at minimum [13]. Thus, the lower limit is set as the value. For k_{R1} and k_{R2}, these ranges are determined using dependence on natural frequency. We confirmed that when both k_{R1} and k_{R2} are below 10^{-1} kN m/rad or above 10^6 kN m/rad simultaneously, natural frequencies in each mode are constant, unaffected by the spring constant. Therefore, ranges of k_{R1} and k_{R2} for the FE model simulation are set as 10^{-1}–10^6 kN m/rad.

Input values of the FE simulation are a set of structural parameters (E_1, E_2, k_{R1}, k_{R2}). These four are sampled 500 times from the parameter space using the Latin hypercube sampling[1]. Output is the live-load displacement at D2 and D4 under the 1 kN load. The maximum value at each location is extracted from the simulation results. Surrogate models for the maximum displacement at D2 and D4 are developed using 500 results of FE model simulations and the Gaussian Process Regression. The performance of the surrogate models is validated using the maximum percentage error of $\lesssim 1\%$. In this way, the displacement ratio of D4 to D2 is estimated at arbitrary structural parameters.

4.2 FE MODEL UPDATE EXECUTION

Using the FE simulations, PDFs of structural parameters are estimated from PDFs of displacement ratio. Prior probability distributions of structural parameters should be set as narrow as possible considering any knowledge of structures and materials [10]. Moreover, k_{R1} and k_{R2} are unimportant and adjustable parameters to match observed results because this paper focuses on only the damage in the girder. Thus, uniform distributions with a narrow range are adopted for k_{R1} and k_{R2}; $\log_{10}(k_{R1}\ [\mathrm{kN\,m/rad}])$ and $\log_{10}(k_{R2}\ [\mathrm{kN\,m/rad}])$ are sampled from the distributions $\mathcal{U}[1,3]$ and $\mathcal{U}[-1,1]$, respectively. These ranges are determined in terms of trial-and-error approach matching natural frequencies measured in the intact scenario. Values of k_{R2} are lower than those of k_{R1} because the A2 bearing is the roller and the A1 bearing is the pin. Namely, it is expected that the spring stiffness in the A2 bearing is lower than that in the A1 bearing. The prior distributions of E_1 and E_2 are set as the uniform distribution with the same range of the parameter space for the FE simulations; E_1, $E_2 \sim \mathcal{U}[0.75E_0, 1.1E_0]$, where E_0 is the nominal value of Young's modulus for steel.

MCMC iterations are 30,000 and burn-in is initial 5,000 iterations. After the MCMC process, sets of accepted structural parameters are obtained. The stationarity and Markov properties in the MCMC process are checked from the autocorrelation function of the parameters' paths. Figure 7 shows estimated PDFs of E_1 and E_2 in the intact and damage scenarios. A way of damage detection from these PDFs is described in the next section.

[1]Note that k_{R1} and k_{R2} are sampled in the logarithmic scale.

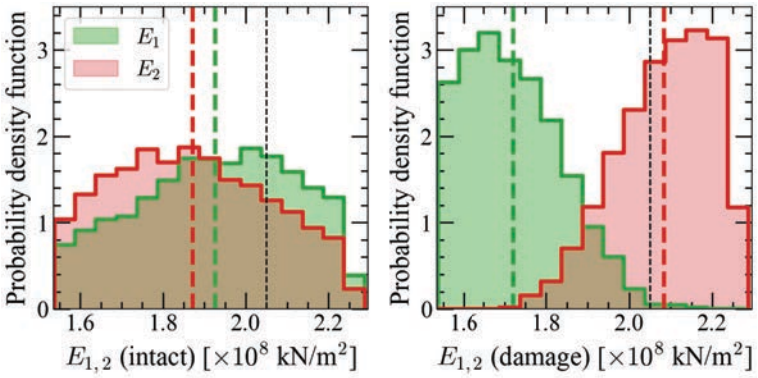

Figure 7: Estimated probability density functions of E_1 and E_2 in the intact and damage scenarios. Thick dashed lines in color are expectations and the thin dashed line is the nominal value of Young's modulus for steel.

Table 1: Expectations and their differences in E_1 and E_2 PDFs.

Scenario	E_1 [$\times 10^8$ kN/m^2]	E_2 [$\times 10^8$ kN/m^2]	$\lvert E_1 - E_2 \rvert$ [$\times 10^8$ kN/m^2]
Intact	1.93	1.87	0.0555
Damage	1.72	2.08	0.363

5 PROBABILISTIC DAMAGE DETECTION

Figure 7 indicates that the overlap area between PDFs of E_1 and E_2 in the damage scenario is much lower than that in the intact scenario. It suggests that the displacement ratio reflects the relative difference (asymmetry) of the flexural rigidity for each half span of the girder. The overlap area in the intact and damage scenarios is 15.5% and 86.6%, respectively. Expectations of the PDFs and their differences between E_1 and E_2 are listed in Table 1. The difference in the damage scenario is also much larger than that in the intact scenario. Considering these results, damage detection is possible by setting a threshold for the overlap area of the PDFs or the difference in their expectations.

Statistical tests for estimated PDFs are also useful in detecting damage. For instance, the Kolmogorov–Smirnov (K–S) test is applied to check the statistical significance of the difference between E_1 and E_2 PDFs. 5% of the significance level is adopted. The p-value of the K–S test in the intact and damage scenarios is 0.054 and 10^{-38}, respectively. Thus, the difference between E_1 and E_2 PDFs in the damage scenario is statistically significant.

Moreover, it is possible to estimate the approximate position of the damage in Figure 7. Any damage in the girder decreases flexural rigidity. Thus, an estimated PDF of Young's modulus in a part of the damaged girder is expected to shift to a lower value. In Figure 7, the PDF of E_1 shows this tendency. Artificial damage is actually in the half span of the girder corresponding to E_1 (cf. Figure 6). Hence, the approximate position of damage in the girder can be estimated as well as damage detection from structural parameters PDFs.

6 CONCLUSIONS

This paper has proposed a damage detection method for bridges using displacement ratio PDF and the FE model update. The main conclusions are as follows.

1. The validity of displacement ratio PDF for BSHM is verified.

2. The results of the FE model update indicate that the displacement ratio mainly reflects a relative difference in flexural rigidity.

3. Estimated PDFs of Young's modulus, as an alternative to flexural rigidity, for each half span of the girder (E_1 and E_2) from displacement ratio show that the overlap area between E_1 and E_2 significantly decreases in the damage scenario. Damage detection is available by setting a threshold of the overlap area or the difference in the expectations of E_1 and E_2 PDFs. Statistical tests are also helpful.

4. Based on the Kolmogorov–Smirnov test, the difference between E_1 and E_2 PDFs in the damage scenario is statistically significant at the significance level of 5%. Thus, artificial damage in the girder is detected at the level.

The proposed method also enables us to quantify damage severity. As damage severity increases, the difference in PDFs of structural parameters from the reference condition becomes significant. Therefore, statistical indices of the distance between two distributions, such as the Kullback–Leibler divergence and the L^1-norm, are promising to quantify damage using estimated structural parameters PDFs.

REFERENCES

[1] M. Yang, "An Integrated Real-Time Health Monitoring and Impact/Collision Detection System for Bridges in Cold Remote Regions," *MPC 15-282*, 2015. [Online]. Available: https://rosap.ntl.bts.gov/view/dot/28782

[2] B. M. Phares, T. J. Wipf, P. Lu, L. Greimann, and M. Pohlkamp, "An experimental validation of a statistical-based damage detection approach," *InTrans Project 08-336*, 2011. [Online]. Available: https://rosap.ntl.bts.gov/view/dot/26134

[3] P. Waibel, O. Schneider, H. B. Keller, J. Müller, O. Schneider, and S. Keller, "A strain sensor based monitoring and damage detection system for a two-span beam bridge," in *Maintenance, Safety, Risk, Management and Life-Cycle Performance of Bridges, Proceedings of the Ninth International Conference on Bridge Maintenance, Safety and Management (IABMAS 2018)*, N. Powers, D. Frangopol, R. Al-Mahaidi, and C. Caprani, Eds., 2018.

[4] A. Döring, P. Waibel, J. Matthes, L. Bleszynski, O. Scherer, H. B. Keller, S. Keller, J. Müller, and O. Schneider, "Ratio-based features for data-driven bridge monitoring and

damage detection," in *Bridge Maintenance, Safety, Management, Life-Cycle Sustainability and Innovations, Proceedings of the Tenth International Conference on Bridge Maintenance, Safety and Management (IABMAS 2020)*, H. Yokota and D. M. Frangopol, Eds., 2021.

[5] J. Mottershead and M. Friswell, "Model updating in structural dynamics: A survey," *Journal of Sound and Vibration*, vol. 167, no. 2, pp. 347–375, 1993.

[6] K. Worden, C. R. Farrar, G. Manson, and G. Park, "The fundamental axioms of structural health monitoring," *Proceedings of the Royal Society A.*, vol. 463, pp. 1639–1664, 2007.

[7] K. F. Alvin, W. L. Oberkampf, K. V. Diegert, and B. Rutherford, "Uncertainty quantification in computational structural dynamics : A new paradigm for model validation: Proceedings of the 16th international modal analysis conference," 1998.

[8] J. Beck and L. Katafygiotis, "Updating models and their uncertainties. i: Bayesian statistical framework," *Journal of Engineering Mechanics*, vol. 124, no. 4, pp. 455–461, 1998, cited by: 1213.

[9] L. Katafygiotis and J. Beck, "Updating models and their uncertainties. ii: Model identifiability," *Journal of Engineering Mechanics*, vol. 124, no. 4, pp. 463–467, 1998, cited by: 332.

[10] M. Nishio, J. Marin, and Y. Fujino, "Uncertainty quantification of the finite element model of existing bridges for dynamic analysis," *Journal of Civil Structural Health Monitoring*, vol. 2, pp. 163–173, 12 2012.

[11] M. W. Vanik, J. L. Beck, and S. K. Au, "Bayesian probabilistic approach to structural health monitoring," *Journal of Engineering Mechanics*, vol. 126, p. 738, 2000.

[12] X. Zhou, C.-W. Kim, F.-L. Zhang, and K.-C. Chang, "Vibration-based bayesian model updating of an actual steel truss bridge subjected to incremental damage," *Engineering Structures*, vol. 260, p. 114226, 2022.

[13] C.-W. Kim, R. Isemoto, T. Toshinami, M. Kawatani, P. McGetrick, and E. J. O'Brien, "Experimental investigation of drive-by bridge inspection," *5th International Conference on Structural Health Monitoring of Intelligent Infrastructure*, 2011.